One Drought and One Volcanic Eruption Influenced the History of China: The Ming Dynasty Mega-drought

Kefan Chen[1], Liang Ning[1,2,3,4*], Zhengyu Liu[5*], Jian Liu[1,2,6], Mi Yan[1,2], Weiyi Sun[1], Linwang Yuan[1], Guonian Lv[1], Longhui Li[1] and Chunhan Jin[1], Zhengguo Shi[4]

[1]Key Laboratory for Virtual Geographic Environment, Ministry of Education; State Key Laboratory Cultivation Base of Geographical Environment Evolution of Jiangsu Province; Jiangsu Center for Collaborative Innovation in Geographical Information Resource Development and Application； School of Geography, Nanjing Normal University, Nanjing, 210023

[2]Open Studio for the Simulation of Ocean-Climate-Isotope, Qingdao National Laboratory for Marine Science and Technology, Qingdao, 266237

[3]Climate System Research Center, Department of Geosciences, University of Massachusetts, Amherst, 01003, United States

[4]State Key Laboratory of Loess and Quaternary Geology, Institute of Earth Environment, Chinese Academy of Sciences, Xi'an, 710063

[5]Department of Geography, The Ohio State University, Columbus, OH 43210, USA

[6]Jiangsu Provincial Key Laboratory for Numerical Simulation of Large Scale Complex Systems, School of Mathematical Science, Nanjing Normal University, Nanjing, 210023

Corresponding author: Liang Ning (ningliangnnu@njnu.edu.cn) & Zhengyu Liu (liu.7022@osu.edu)

Key Points:

- Main point #1: The decline of Ming Dynasty (1644) is contributed greatly by the Ming Dynasty Mega-drought (MDMD) in 1637-1643
- Main point #2: The MDMD is triggered by a natural drought event in 1637 and is then intensified and extended by the strong volcanic eruption in 1641.
- Main point #3:The intensified MDMD is related to the weakening of land–ocean thermal contrast, West Pacific Subtropical High and soil moisture.

Abstract

The Ming Dynasty Mega-drought (MDMD) (1637-1643) occurred at the end of Ming Dynasty and is the severest drought event in China in the last millennium. This unprecedented drought contributed significantly to the collapse of the Ming Dynasty in 1644, casting profound impacts on Chinese history. Here, the physical mechanism for the MDMD is studied. Based on paleoclimate reconstructions, we hypothesize that this drought was initially triggered by a natural drought event starting in 1637, and was then intensified and extended by the tropical volcanic eruption at Mount Parker in 1641. This hypothesis is supported by the case study of the Community Earth System Model-Last Millennium Experiment archive as well as sensitivity experiments with volcanic forcing superimposed on natural drought events. The volcano-intensified drought was associated with a decreased land–ocean thermal contrast, a negative soil moisture response and a weakening and eastward retreating West Pacific Subtropical High.

Keywords

Chinese history; Paleoclimate; Ming Dynasty Mega-drought; volcanic eruption; climate modeling

Plain Language Summary

The collapse of Ming Dynasty at 1644, and in turn, the historical transition from Ming Dynasty to Qing Dynasty significantly changed the Chinese history into a long period of conservative policy. The collapse of Ming Dynasty at 1644 is contributed greatly by the Ming Dynasty Mega-drought (MDMD) (1637-1643). In this study, based on paleoclimate reconstructions and climate modelling, we show that the MDMD is triggered by a natural drought event, and is then intensified and extended by the strong volcanic eruption at Mt. Parker in 1641. This "superposition" mechanism of MDMD and the spatiotemporal characteristics of this drought is reproduced by our volcanic sensitivity experiments with volcanic forcing superimposed on natural drought events, and the results demonstrate that the explosion of Mt. Parker at the end of a natural drought event amplified and extended the drought for 3 years, generating the mega-drought. The volcano-prolonged drought is associated with the failure of EASM, which is directly caused by the decreasing of land–ocean thermal contrast after volcanic eruption, and indirectly influenced by negative soil moisture feedback as well as weakening and eastward retreating of West Pacific Subtropical High (WPSH).

1 Introduction

The Ming Dynasty (AD 1368-1643) is one of the most important historical periods in Chinese history, and is known for its flourish of socioeconomy and germination of capitalism (Cai, 1965). The collapse of the Ming Dynasty and the subsequent transition to Qing Dynasty (AD 1644-1911), which reversed to conservative policies, is critically influenced by the 7-year long Ming Dynasty Mega-drought (MDMD) in 1637-1643, during which food crisis, famines, plagues and wars prevailed (Shen et al., 2007; Cook et al., 2010; Zheng et al., 2014a). As the severest drought event in eastern China in the past millennium, the MDMD aggravated the

national fiscal deterioration and the vulnerability of social structures, casting profound impacts on the history of China (Ge et al., 2012; Zheng et al., 2014b; Peng et al., 2014).Therefore, the mechanisms triggering and maintaining MDMD has attracted profound attentions from history, climatology, sociology communities(Zhang, 2004; Shen et al., 2007).

The occurrence of severe droughts like the MDMD over China has stimulated much effort in investigating their mechanisms(Zhang and Zhou, 2015), which is of great value for drought prediction and disaster alleviation in the future. Previous studies demonstrated that droughts in eastern China is associated primarily with the weakening of East Asia summer monsoon (EASM) (Ding, 1994; Cook wt al., 2010), which is caused often by internal climate variability (Ma, 2007; Ning et al., 2019b) through changes in western Pacific subtropical high (WPSH) (Zhou et al., 2005; Man et al., 2012) and sea surface temperature over the North Pacific and tropical Pacific (Zhang et al., 2015). Meanwhile, external forcing, notably, volcanic eruption, can also drive serious rainfall deficit in eastern China (Shen et al., 2007; Shen et al., 2008; Man and Zhou, 2014) by either enhancing the Atlantic Multidecadal Oscillation (AMO) (Ning et al., 2019a; Kundsen et al., 2014) or inducing El Niño/Southern Oscillation (ENSO) (Adams et al., 2003).

However, the mechanism triggering and maintaining the MDMD has remained exclusive (Zheng et al., 2014a). How did this mega drought event become so severe and persist so long? In this paper, based on paleoclimate reconstructions and modeling, we show that the MDMD was caused by the combined effect of internal climate variability and external forcing. The MDMD was triggered initially by a natural drought event, and was then intensified significantly by the volcanic eruption at Mount Parker in South Philippines in 1641.

2 Materials and Methods

2.1 Sensitivity experimental design

In this paper, the evolution process of the MDMD was reproduced by volcanic sensitivity experiments based on CESM1.0.3 (Hurrell et al., 2013) version T31_g37. The monthly data simulated by CESM has a ~3.75 resolution for atmosphere and land components as well as the ocean and sea ice components. Firstly, we ran a 2400-year control experiment basing on the initial condition of AD1850 and selected 10 initial conditions from the last 2000 years of the control run, as the first 400 years are for spinning up.

Subsequently, ten 50-year control experiments were performed based on these 10 initial conditions. 15 drought cases are then extracted from the 10 runs, representing the first several years of the MDMD that was triggered by internal variability. After that, The Ice-core based Volcanic Index 2 reconstructed by Gao, et al (2012) is used as the volcanic forcing to drive the model which is the only external forcing during the integrations simulated in the runs. The volcanic aerosol spanning from January 1641 to December 1645 (Fig. S5) was imposed to the last year of each of the 15 drought cases in order to simulate the influences of the volcanic eruption at Mt. Parker at the end of this drought. Both control and volcanic sensitivity experiments were run in parallel with the same initial condition.

2.2 Definition of the Ming Dynasty Mega-drought

According to literature records, the catastrophic MDMD primarily took place in AD 1637-1643, during which drought conditions over the eastern China, especially the Yellow River basin

and Yangtze-Huaihe river areas (Jiang-Huai area), were the severest (Zheng et al., 2014a; Zhang et al., 2005). Hence, following previous studies, the region of the North China Plain and Jiang-Huai area (105°-120°E, 32°-40°N) is selected as the study region in this paper (Fig. S1). Furthermore, taking different definitions of drought from previous studies (Stevenson et al., 2015; Ning et al., 2019a; Ault et al., 2016), the drought is defined as negative precipitation anomalies lasting for about 5 consecutive years with maximum precipitation anomalies larger than 1 standard deviation over eastern China.

2.3 Superposed Epoch Analysis

The Superposed Epoch Analysis (SEA) is a powerful composite technique widely used to reveal the volcanic impacts on climate changes (Admas et al., 2003; Hartmann et al., 2016). In this paper, through the application of SEA, we evaluated the composite response of 15 drought cases to the same volcanic forcing. To the 15 cases from control and volcanic sensitivity experiments, the last year of the natural drought (the same as the year of volcanic eruption) is considered as the key time of SEA. Then, a 21-yr window centred on the eruption year with 10 years before and 10 years after the eruption was picked up from each of the 15 members. The eruption year is marked as year 0 and the years before (after) the eruption are marked as year -1 (1), year -2 (2), etc. Finally, precipitation anomalies of the 15 cases were averaged and all anomalies are calculated with respect to the long term mean of the entire control simulation.

3 Data

To show the severity of the Ming Dynasty Mega-drought in paleoclimate records, the reconstructed data used in this paper include the Dry and Wet Index (DWI) time series from 500-2000 based on historical records (Zheng et al., 2006) and the summer precipitation reconstructed from tree-ring chronology and historical documents for period 1471-2014 (Shi et al., 2018). The reconstructed precipitation has a ~2 degree resolution and covers the area of Asia (-8.75°S-55.25°N, 61.25°E-143.25°E). The sensitivity experiments use the transient evolution of reconstructions on volcanic sulfate aerosol from ice records (Gao et al., 2012) as external volcanic forcing. The monthly precipitation data from control experiment (CTRL) and 13 all-forcing experiments (ALL) extending from 850-1850 from the CESM-LME archive are also used to investigate the influences on the precipitation over the eastern China from volcanic eruptions in the past millennium. The simulations derived from the CESM-LME archive has a ~2 degree resolution for atmosphere and land components (Otto-Bliesner et al., 2015).

4 Results

4.1 Evolution characteristics of MDMD

The MDMD can be seen in both reconstructions of the Dry and Wet Index (DWI) and the regional mean summer precipitation (JJA) in eastern China during the period 1350-1850 (Shi et al., 2018), both of which show a significant decrease in AD 1637-1645. The decrease magnitude is close to 3 times standard deviation and was the largest in the past 500 years (Figs. 1a, 1b, 2a, 2b). According to reconstructions, there was no strong external forcing event, such as volcanic eruption, at or immediately preceding the onset of the MDMD at 1637 (Figs.1c, 2c). The precipitation minimum, which occurred in the middle of MDMD around AD 1641 coincides

closely with the year of the eruption of volcano at MT. Parker (Figs. 1c, 2c) and the dry condition persisted ~4 years after the volcanic eruption. These observational features lead us to hypothesize a "superposition" mechanism (volcanic forcing superposed on internal variability) for MDMD: MDMD was triggered by a natural drought event in 1637, and was then amplified and extended by the MT. Parker volcanic eruption from 1641 to 1644, generating a 7-year mega-drought event.

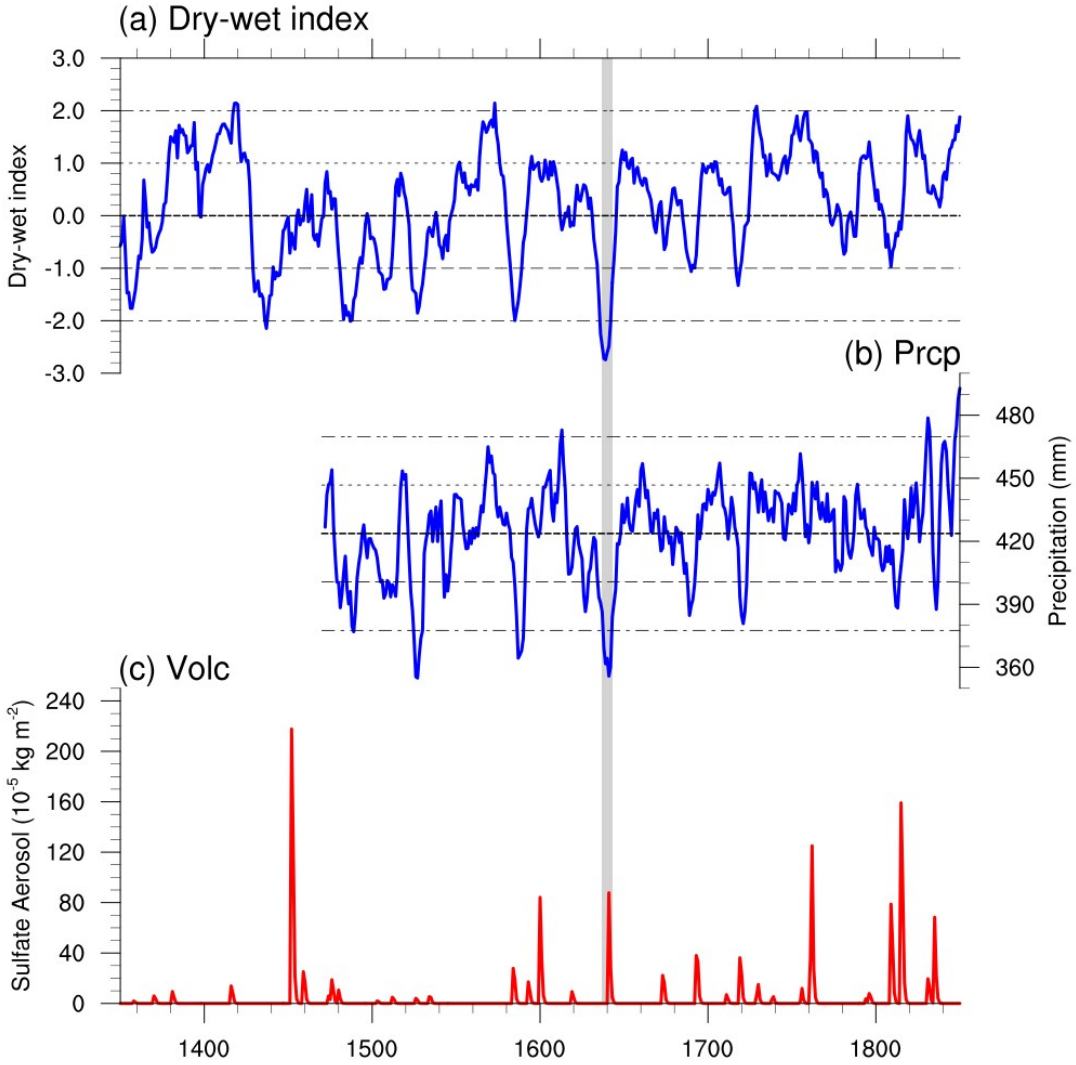

Figure 1. The MDMD in reconstructions. (a) The reconstructed DWI from AD 1350-1850 (10-year running mean); (b) The reconstructed 5-year running mean summer (JJA) precipitation over the North China Plain and the Yangtze and Huaihe river areas (Fig. S1) between AD 1471 and 1850 (Unit: mm); (c) The reconstructed sulphate aerosol in period of AD 1350-1850 (Unit:10^{-5}Kg/m^2).

4.2 The Cause of MDMD

4.2.1 Different roles of internal variability, volcanic eruption, and their combination

Our proposed superposition mechanism is supported first by the analysis of the 13 all-forcing experiments from the CESM Last Millennium Ensemble Project (CESM-LME) archive

(Otto-Bliesner et al., 2015). The drought impact of the MT. Parker volcanic eruption on the regional precipitation over eastern China is confirmed by the significant decrease following the eruption at 1641 in the ensemble mean precipitation (Fig. S2i). Nevertheless, consistent with our observational analysis above (Fig. 2a-c), this model precipitation response also shows that MT. Parker volcanic eruption was not the trigger for MDMD, because the MT. Parker eruption only forces the drought immediately after 1641, already half way into MDMD. This leaves the triggering mechanism to a natural drought event associated with internal climate variability, which is similar to droughts in other regions (Stevenson et al., 2015; Ault et al., 2018; Ning et al., 2019a). Meanwhile, MDMD is unlikely to be caused by the natural variability alone. This is demonstrated in a 2000-member red noise Monte Carlo test for the 1000 years of CESM control run (Fig. S4 and SI Text1). In 1000 years, there is only 10% occurring probability of one mega-drought of 7-year length and above 3-sigma intensity as a natural event. In comparison, for natural drought with a 7-year length and above 2-sigma intensity, the occurring probability of 1 or 2 droughts is 30%. Therefore, a mega-drought like MDMD has a small occurring probability if merely caused by internal variability. The superposition of volcanic impact on a natural drought should enhance the occurring probability of a mega-drought event like MDMD.

The triggering drought event and the extension by volcanic eruption can be first examined by comparing the drought events with and without volcanic influence. In the CESM-LME all-forcing experiments, there are 11 natural drought events that occurred more than 3 years prior to a volcanic eruption in the last millennium (thick dashed colored lines in Figs. S3d-g, i, k, l and SI Text2), similar to MDMD (Fig. 2a-c). The ensemble mean of these events shows a sharp decline of summer precipitation after the eruption and then an extension of drought for another ~3 years (Fig. 2d); furthermore, within these 11 events, the drought magnitude is significantly amplified in 7 cases (Fig. S3 and SI Text2), as in MDMD. By contrast, as a background, the natural drought events that are not followed by volcanic eruptions shows a weaker and shorter drought in the ensemble mean (Fig. 2e and SI Text2). For the volcanic events that are not proceeded by droughts for 3 years, the ensemble mean precipitation response shows a much weaker and shorter response (Fig. 2f). This comparison demonstrates that volcanic eruption can amplify and extend a natural drought event. The reconstructed spatiotemporal distribution of the MT. Parker volcanic aerosol (Fig. S5) suggests that the impact of volcanic eruption in 1641 can be sustained for about 3 years. This coincides with the approximate 3-year persistence of the MDMD after the eruption of MT. Parker. Therefore, our analysis of the CESM-LME ensemble supports the superposition mechanism hypothesis for MDMD.

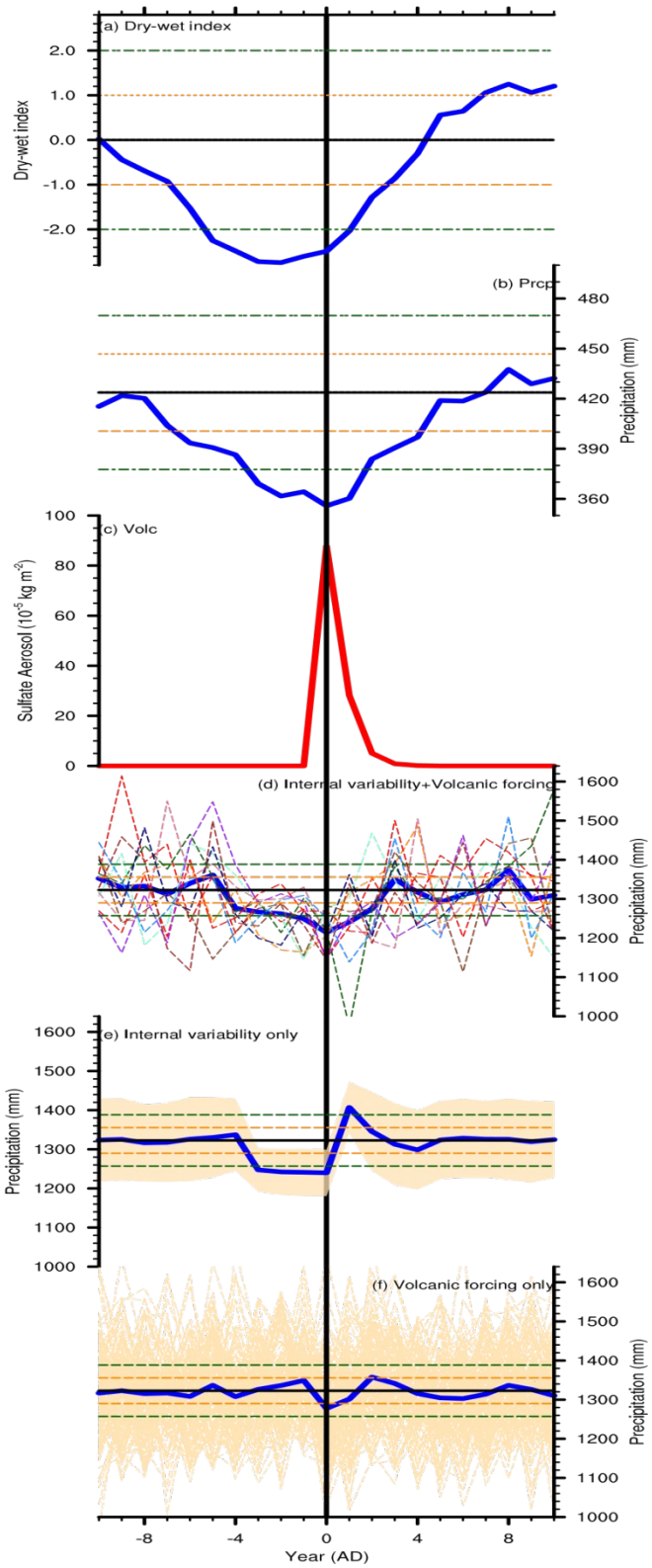

Figure 2. Paleoclimate reconstructions of the MDMD and the precipitation anomalies with and without volcanic influences from the 13 simulations of CESM-LME. (a) The reconstructed DWI during the period of AD 1631-1651; (b) The 5 year running mean reconstructed summer (JJA) precipitation over the eastern China during the period AD 1631-1651 (Unit: mm); (c) The reconstructed sulphate aerosol during period of AD

1631-1651 (Unit: 10-5Kg/m2); (d) The ensemble mean summer (MJJAS) precipitation (blue line) centred with volcanic eruptions (>25Tg, Fig S2) that composite 11 droughts triggered initially by natural variability (persist more than 3 years before the eruptions) and then strengthened by volcanic eruptions from the 13 all-forcing CESM-LME simulations during the past millennium, and the 11 ensemble members (coloured thick dashed lines, Fig. S3); (e) similar to (d), but all the 414 ensemble members (yellow shading area) are centred with volcanic forcing only, without droughts due to natural variability before volcanic eruptions; (f) Similar to (d) but all of the 155 ensemble members (yellow dash lines) are centred with the last year of natural drought events due to natural variability (persist more than 3 years) only, without volcanic forcing. The yellow and green dashed lines indicate the ±1 and ±2 standard deviations, respectively.

4.2.2 Volcanic sensitivity experiments

We further validate the superposition mechanism in an ensemble of specifically designed sensitivity experiments in CESM. First, 15 drought events induced by natural variability are selected from 500 years of control simulation (with no external forcing) with each event of a duration of 3-5 years, which roughly equals the first half period of MDMD between 1637 and 1641 (Fig. 3a). Then, the volcanic forcing of Mt. Parker volcanic eruptions for 1641-1645 (Fig. S5), was imposed starting at the end of the 15 natural drought events (Fig. 3b). Finally, the Superposed Epoch Analysis (SEA) is used on the annual precipitation anomalies of these 15 cases for both the control experiments and sensitivity experiments. A comparison of the control and sensitivity experiments shows a sharp contrast (Fig. 3a vs. b). Without volcanic forcing, the drought events tend to last for about 5 years ending with a wet event (Fig. 3a, Fig. S6a). The Mt. Parker volcanic eruption, however, suppresses this otherwise wet event and, moreover, produces a prolonged drought, with the negative precipitation anomaly extending up to 3 years after the volcanic eruption, which are significant ($p<0.05$) based on the student t-test (Fig. 3b, S6b). In the 4th year after eruption, rainfall mostly recovers, consistent with the MDMD in reconstruction (Fig. 2a-c). The difference of annual precipitation between the sensitivity and control experiments in the same period shows strong negative anomalies after volcanic eruption, indicating a strong suppression effect of volcanic eruptions on precipitation after overwhelming an otherwise wet event (Fig. S7). Furthermore, compared with annual mean precipitation, the summer precipitation, which accounts for the largest proportion of the annual rainfall (Fig. S8), shows larger precipitation decrease averaged from the eruption year to the third year after volcanic eruption (-0.38 mm/day, over 1 standard deviation). These experiments highlight the roles of the natural variability and volcano in triggering and enhancing/extending the drought event, respectively, and therefore, further support the superposition hypothesis.

The sensitivity experiments also suggest that the unprecedented magnitude of the MDMD can be reasonably achieved in the model simulations. Although the ensemble-averaged magnitude of droughts after eruption in the sensitivity experiments (about 1 standard deviation, Figs.3b, S8) is not as large as reconstruction (close to 3 standard deviations, Figs.2a, b), the real world MDMD, however, is a single realization. In a single realization, the drought event forced by the volcano can reach significantly higher amplitude than the ensemble mean. For example, in the sensitivity experiments here, although the ensemble mean summer drought precipitation after volcanic eruption is only 1-sigma deviation, 5 of the 15 cases achieve a magnitude over 2-sigma deviation in the first 3 years after the volcanic forcing (thick dashed coloured lines in Fig. S8d), approaching the MDMD level, while none reaches 2-sigma level without the volcanic forcing (Fig. S8c for negative years). It should be noted that the intensities of the initial drought events selected from the control runs for sensitivity experiments are not sufficiently strong. Otherwise, a

single realization is more likely to reach an even higher amplitude comparable with the reconstructed MDMD.

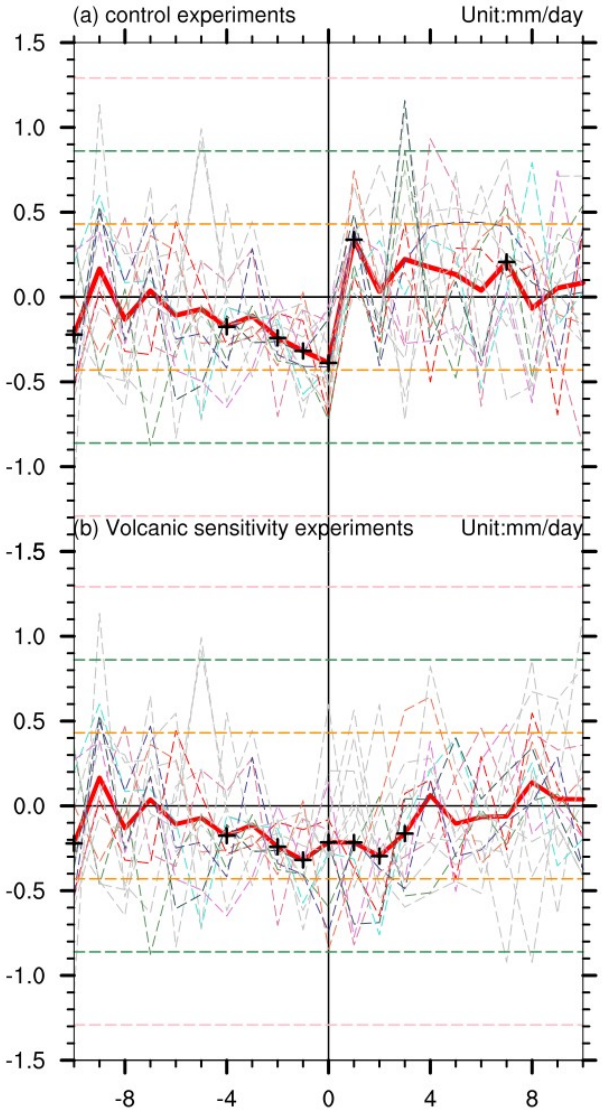

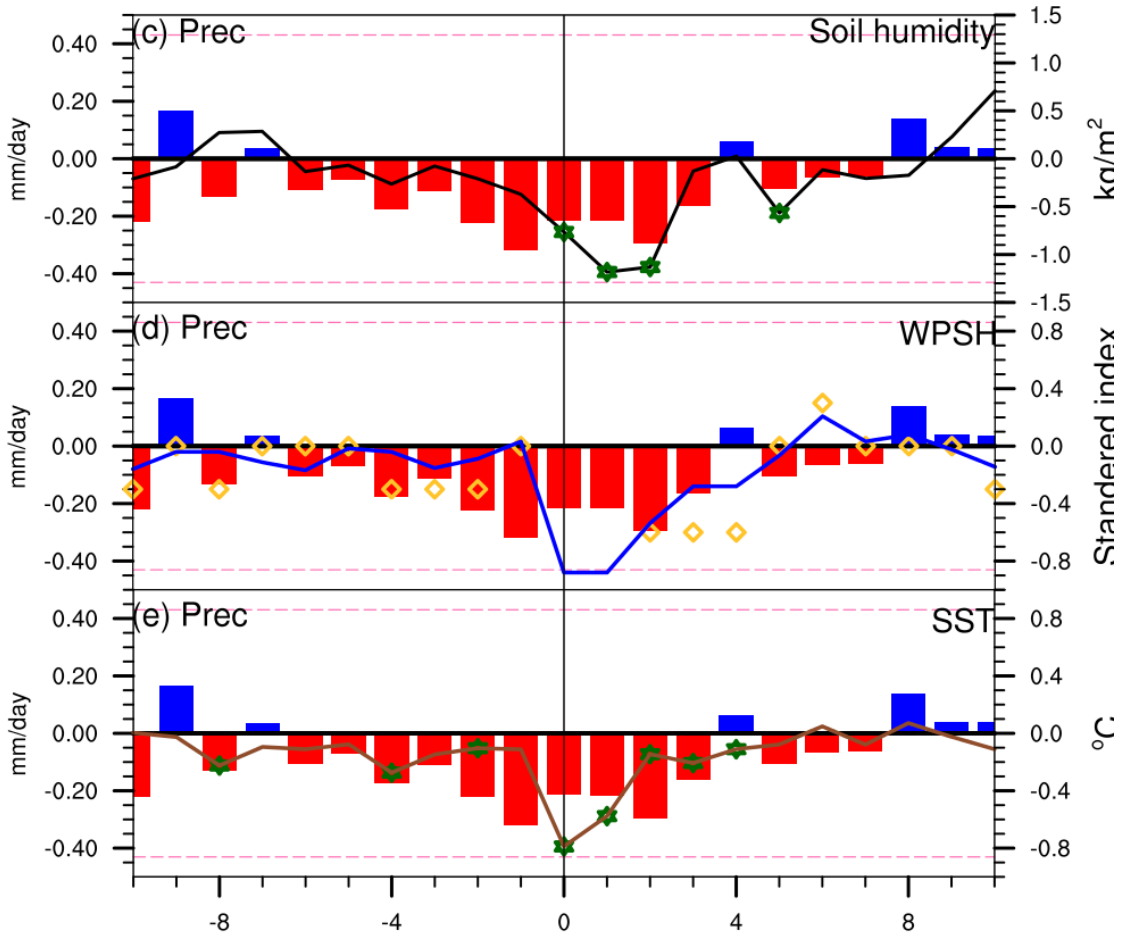

Figure 3. The superposed echo analysis of the annual mean precipitation anomalies (unit: mm/day) from the control experiments (a) and sensitivity experiments (b); The symbols of "+" indicate that the anomalies are significant at 95% level based on Student t-test. The pink, green and orange dash lines indicate the ±1, ±2 and ±3 standard deviation, respectively;
(c)-(e) The superposed echo analyses of the precipitation anomalies (bars, left y-axis, unit: mm/day), which is the same as (b); (c) soil moisture anomalies over eastern China (black line, right y-axis, unit: kg/m^2); (d) variations of WPSH's west ridge point (yellow diamond, right y-axis, standardized), area covered by WPSH (blue line, right y-axis, standardized) from the volcanic forcing sensitivity experiments; (e) SST anomalies over the northwestern Pacific key region (123°E-150°E, 15°N-30°N) (brown line, right y-axis, unit: °C). The green "*" in (c)-(e) indicate that the anomalies are significant at 95% level based on Student t-test.

4.3 Mechanisms behind the influences of volcanic eruption on the MDMD

Mega-droughts over the eastern China are usually caused by the weakening of East Asian summer monsoon (EASM) (Cook et al., 2010). After volcanic eruption, the eastern China is dominated by an anomalously positive SLP and northerly wind (Fig. S10), with rainfall decreasing over the Yangtze River and North China region (Fig. S11). The EASM does not recover until 3 years after the eruption (Figs. S10, 11).

Volcanic eruption reduces the temperature differences between land and ocean, and then directly weakens EASM. After the volcanic eruption, both the surface air temperature (SAT) over the eastern China and the sea surface temperature (SST) of adjacent ocean areas decreased (Fig. 4). The SST responded to the volcano-induced radiative forcing more slowly than the SAT in the first two years after volcanic eruptions, because of its larger thermal capacity. Therefore,

the magnitude of SAT decrease is larger than SST by about 0.5°C in summer on the eruption year. This temperature difference reduces the land-sea thermal contrast and generates a higher SLP over land, which then reduces the southerly EASM wind and the corresponding moisture transport, and, eventually, EASM rainfall over eastern China, consistent with findings in previous studies (Man et al., 2014). The cold SST along the east coast of China during the MDMD (Figs. 3e and S12) may also contribute to the weakened EASM by reducing the adjacent moisture source into eastern China.

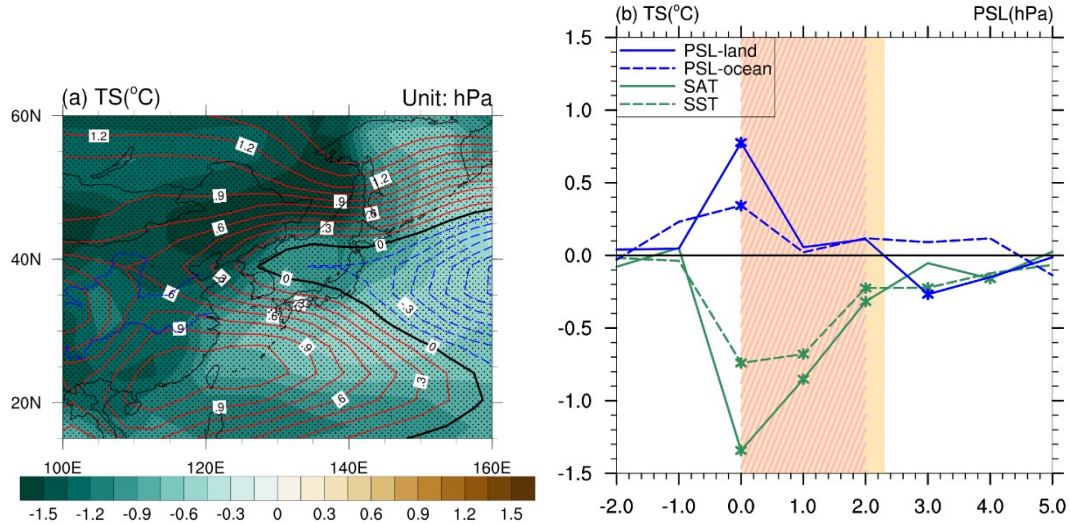

Figure 4. (a) The spatial pattern of summer (May-September) temperature (a, unit: °C) at the year of volcanic eruption (0 years). (b) The area-mean sea surface temperature (SST, dashed green line unit: °C), surface air temperature (SAT, unit: °C, green solid line) and sea level pressure (SLP, unit: hPa) over eastern China (20-50°N, 90-120°E; blue solid line) and surrounding oceans (20- 50°N, 125-150°E; blue dashed line). The yellow shaded area covers the period when the SST is higher than the SAT after the volcanism. The pink shaded area covers the period when the SLP over land is greater than the ocean after volcanic eruption. The symbol of "*" indicates that the results of that year has passed the Student-T-test.

The weakening EASM by volcanic eruption is also associated with the weakening WPSH. In the first two years after volcanic explosion, the WPSH weakens (Fig. S13) and retreats eastward (Figs. 3d and S12), accompanied by anomalous northwesterly wind over eastern China (Fig. S12) which further weakens the EASM (Huang et al., 1991). The weaker WPSH does not recover until year-5, and the variations of WPSH coincide with the changes of precipitation anomalies in eastern China. Additionally, the weakening EASM by volcanic forcing may also be amplified by soil moisture feedback. Volcanic eruption reduces rainfall and, in turn, soil moisture, as seen in the negative soil moisture response that lasts for 3 years after the volcanic eruption (Fig. 3c). Meanwhile, soil moisture is significantly correlated with the precipitation anomalies not only after the eruption, but also before the eruption because of the triggering natural drought event. The soil moisture depletion preceding the volcano forcing may provide an precondition for positive soil moisture feedback (Koster et al., 2004; Liu et al., 2006) on the rainfall decrease, amplifying the impact of volcanic eruption.

5 Conclusions

Our observational and modelling study suggest that the natural drought event starting at 1637 is amplified by the Mt. Parker volcanic eruption in 1641, generating the unprecedented

MDMD that has severely influenced the history of China. The MDMD is therefore not only a well-known event due to its social and historical impacts, but also a prototype of climate event that is caused by the combined effect of internal climate variability and external forcing. The volcano-intensified drought is associated with a weakening of EASM after volcanic eruption, which is directly caused by decreased land–ocean thermal contrast, and indirectly influenced by negative soil moisture feedback as well as weakening and eastward retreating of West Pacific Subtropical High (WPSH). The causes of MDMD highlight the necessity of further investigations of climate changes from the unified perspective of internal variability and external forcing for the past and future.

Acknowledgments

This study was jointly supported by the National Basic Research Program of China (Grant No. 2016YFA0600401), the National Natural Science Foundation of China (Grant Nos. 41971021, 41971108, 41671197, and 41631175), Open Funds of State Key Laboratory of Loess and Quaternary Geology, Institute of Earth Environment, Chinese Academy of Sciences (SKLLQG1820).

Dataset of the reconstructed DWI time serie0-s for this research is available through Zheng et al. 2006, and the reconstructed gridded summer precipitation is available through Shi et al. 2017. The ice-core based volcanic aerosol is available through Gao et al. 2008. The model information is available through Otto-Bliesner et al. 2015. The simulated results are underway. We plan to archive our simulated data on National Climate Data Center (NCDC) and have temporarily upload a copy of our simulated data as Supporting Information for review purposes.

References

1. Adams, J. B., Mann, M. E. & Ammann, C. M. (2003), Proxy evidence for an El Niño-like response to volcanic forcing. *Nature* **426**, 274-278, doi:10.1038/nature02087.

2. Ault, T. R., Mankin, J. S., Cook, B. I. & Smerdon, J. E. (2016), Relative impacts of mitigation, temperature, and precipitation on 21st-century megadrought risk in the American Southwest. *Science Advances* **2**, e1600873, doi:10.1126/sciadv.1600873.

3. Ault, T. R. *et al.* (2018), A Robust Null Hypothesis for the Potential Causes of Megadrought in Western North America. *Journal of Climate* **31**, 3-24, doi:10.1175/jcli-d-17-0154.1.

4. Cai, M. B. (1965), Encyclopedia of Chinese History. *People's Press, Beijing*.

5. Cook, E. R. *et al.* (2010), Asian monsoon failure and megadrought during the last millennium. *Science* **328**, 486-489, doi:10.1126/science.1185188.

6. Ding, Y. (1994), Monsoons over China. *Atmospheric and Oceanographic Sciences Library* **16**.

7. Gao, C., Robock, A. & Ammann, C. (2012), Volcanic forcing of climate over the past 1500 years: An improved ice. *Journal of Geophysical Research* **117**, D16112, doi:10.1029/2008JD010239.

8. Ge, Q., Zheng, J., Hao, Z. & Liu, H. (2013), General characteristics of climate changes during the past 2000 years in China. *Science China Earth Sciences* **56**, 321-329, doi:10.1007/s11430-012-4370-y.

9. Hartmann, D. L. (2016), Compositing or Superposed Epoch Analysis. *Compositing* **552**, 38-40.

10. Hurrell, J. W. *et al.* (2013), The Community Earth System Model: A Framework for Collaborative Research. *Bulletin of the American Meteorological Society* **94**, 1339-1360, doi:10.1175/bams-d-12-00121.1.

11. Huang, R. & Sun, F. (1991), Impacts of the Tropical Western Pacific on the East Asian Summer Monsoon. *Journal of the Meteorological Society of Japan* **70**, 244-256.

12. Koster, R. D. *et al.* (2004), Regions of strong coupling between soil moisture and precipitation. *Science* **305**, 1138-1140, doi:10.1126/science.1100217.

13. Knudsen, M. F., Jacobsen, B. H., Seidenkrantz, M.-S. & Olsen2, J. (2014), Evidence for external forcing of the Atlantic Multidecadal Oscillation since termination of the Little Ice Age. *Nature Communications* **5**.

14. Liu, Z., Notaro, M., Kutzbach, J. & Liu, N. (2006), Assessing Global Vegetation–Climate Feedbacks from Observations. *Journal of Climate* **19**, 787-814, doi:10.1175/jcli3658.1.

15. Ma, Z. (2007), The interdecadal trend and shift of dry/wet over the central part of North China and their relationship to the Pacific Decadal Oscillation (PDO). *Chinese Science Bulletin* **52**, 2130-2139, doi:10.1007/s11434-007-0284-z.

16. Man, W., Zhou, T. & Jungclaus, J. H. (2012), Simulation of the East Asian Summer Monsoon during the Last Millennium with the MPI Earth System Model. *Journal of Climate* **25**, 7852-7866, doi:10.1175/jcli-d-11-00462.1.

17. Man, W. & Zhou, T. (2014), Response of the East Asian summer monsoon to large volcanic eruptions during the last millennium. *Chinese Science Bulletin* **59**, 4123-4129.

18. Man, W., Zhou, T. & Jungclaus, J. H. (2014), Effects of Large Volcanic Eruptions on Global Summer Climate and East Asian Monsoon Changes during the Last Millennium: Analysis of MPI-ESM Simulations. *Journal of Climate* **27**, 7394-7409, doi:10.1175/jcli-d-13-00739.1.

19. Ning, L., Liu, J. & Sun, W. (2017), Influences of volcano eruptions on Asian Summer Monsoon over the last 110 years. *Scientific reports* **7**, 42626, doi:10.1038/srep42626.

20. Ning, L. *et al.* (2017), Variability and Mechanisms of Megadroughts over Eastern China during the Last Millennium: A Model Study. *Atmosphere* **10**, 7, doi:10.3390/atmos10010007.

21. Ning, L., Liu, J., Bradley, R. S. & Yan, M. (2019b), Comparing the spatial patterns of climate change in the 9th and 5th millenniaBP from TRACE-21 model simulations. *Climate of the Past* **15**, 41-52, doi:10.5194/cp-15-41-2019.

22. Otto-Bliesner, B. L. *et al.* (2015), Climate Variability and Change since 850 C.E.: An Ensemble Approach with the Community Earth System Model (CESM). *Bulletin of the American Meteorological Society* **97**, 150807114607005, doi:10.1175/BAMS-D-14-00233.1.

23. Peng, Y., Shen, C., Cheng, H. & Xu, Y. (2013), Modeling of severe persistent droughts over eastern China during the last millennium. *Climate of the Past* **9**, 6345-6373, doi:10.5194/cp-10-1079-2014.

24. Shen, C., Wang, W.-C., Hao, Z. & Gong, W. (2007), Exceptional drought events over eastern China during the last five centuries. *Climatic Change* **85**, 453-471, doi:10.1007/s10584-007-9283-y.

25. Shen, C., Wang, W.-C., Hao, Z. & Gong, W. Characteristics of anomalous precipitation events over eastern China during the past five centuries. *Climate Dynamics* **31**, 463-476, doi:10.1007/s00382-007-0323-0 (2008).

26. Stevenson, S., Timmermann, A., Chikamoto, Y., Langford, S. & DiNezio, P. (2015), Stochastically Generated North American Megadroughts. *Journal of Climate* **28**, 1865-1880, doi:10.1175/jcli-d-13-00689.1.

27. Shi, H., Wang, B., Cook, E. R., Liu, J. & Liu, F. (2018), Asian Summer Precipitation over the Past 544 Years Reconstructed by Merging Tree Rings and Historical Documentary Records. *Journal of Climate* **31**, 7845-7861, doi:10.1175/jcli-d-18-0003.1.

28. Zhang, D. (2005), Severe drought events as revealed in the climate records of China and their temperature situations over the last 1000 years. *Acta Meteorologica Sinica* **19**, 485-491.

29. Zhang, L. & Zhou, T. (2015), Drought over East Asia: A Review. *Journal of Climate* **28**, 3375-3399, doi:10.1175/jcli-d-14-00259.1.

30. Zheng, J. *et al.* (2014a), How climate change impacted the collapse of the Ming dynasty. *Climatic Change* **127**, 169-182, doi:10.1007/s10584-014-1244-7.

31. Zheng, J., Hao, Z., Ge, Q. & Fang, X. (2014b), Several characteristics of extreme climate events during past 2000 years in China. *PROGRESS IN GEOGRAPHY* **33**, 3-12, doi:10.11820/dlkxjz.2014.01.001.

32. Zheng, J., Wang, W.-C., Ge, Q., Man, Z. & Zhang, P. (2006), Precipitation Variability and Extreme Events in Eastern China during the Past 1500 Years. *Terrestrial Atmospheric and Oceanic Sciences* **17**, 579-592.

33. Zhou, T.-J. & Yu, R. (2005), Atmospheric water vapor transport associated with typical anomalous summer rainfall patterns in China. *Journal of Geophysical Research* **110**, D08104, doi:10.1029/2004jd005413.

Supplementary Information for

One Drought and One Volcanic Eruption Influenced the History of China: The Ming Dynasty Mega-Drought.

Supplementary Information Text

1. **Computing method of red noise.** Firstly, a 1000-year white noise origin was generated randomly basing on a normal distribution using the function "random_normal" in the NCAR Command Language (NCL). Then the red noise is derived using the white noise series as well as the auto-correlation of the 1000-year regional annual rainfall time series over East China (105°-120°E, 32°-40°N) in the Community Earth System Model-Last Millennium Ensemble Project (CESM-LME) control run without external forcing. The computing formula of red noise is: $Red_0=White_0$, $Red_{i+1}=R*Red_i+(1-R^2)^{1/2}*White_{i+1}$ ("Red" is the time series of red noise; "White" is the time series of white noise; "R" is the autocorrelation coefficient calculated by the function esacr (x, mxlag) in NCL; "i" is the subscript).

2. **Drought events with and without volcanic eruptions from CESM-LME.** According to the reconstructed volcanic aerosol (Gao et al., 2012) during AD 850-1850, there exist 17 volcanic eruptions with magnitudes larger than 25Tg (Fig. S7). In the 13 individual all-forcing simulations from CESM-LME (Otto-Bliesner et al.,2015), there are 11 drought events occurred more than 3 years prior to these 17 volcanic eruptions in the total 17*13 cases (Fig. S3, 1 drought event in 1258, 1275, 1452 and 1641 respectively; 2 drought events in 1284 and 1693 respectively; 3 drought events in 1227). Among these 11 cases, 1 drought event in 1452, 1 drought event in 1227, 2 drought events in 1284, 1 drought event in 1641 and 2 drought events in 1693 are prolonged by volcanic eruptions, which is similar to the Ming Dynasty Megadrought. On account of this, there are 55 drought events occurred only 1 or 2 years before volcanic eruption, while 155 cases are centred with volcanic forcing only, without droughts due to natural variability before volcanic eruptions in the total 13*17 cases. Furthermore, in the past millennium, there are 414 cases centred with droughts due to natural variability (persist more than 3 years) only, without volcanic forcing.

Fig. S1.

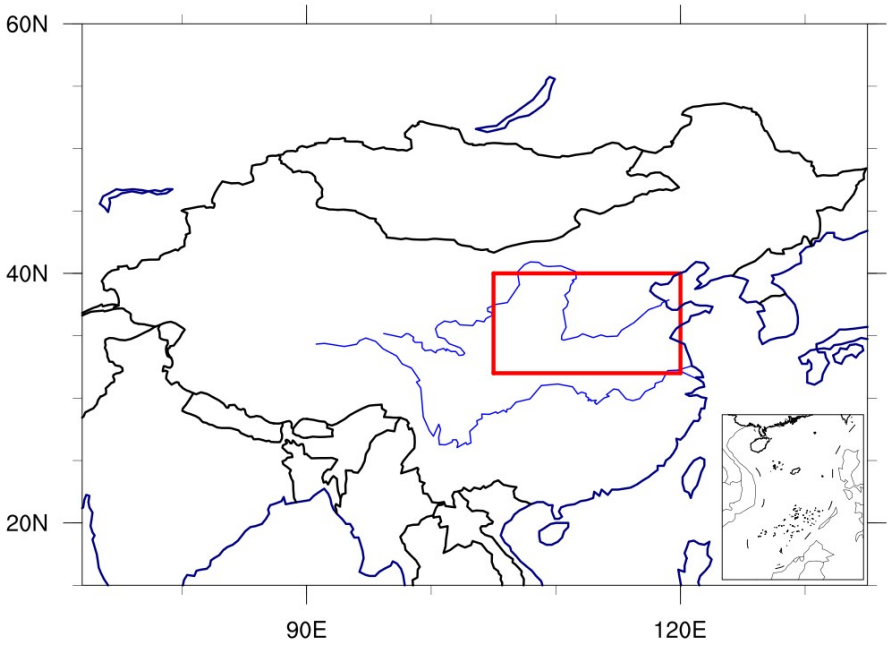

Fig. S1. The region of Yellow River basin and Yangtze-Huaihe river areas (Jiang-Huai area) (105°-120°E, 32°-40°N)

Fig. S2.

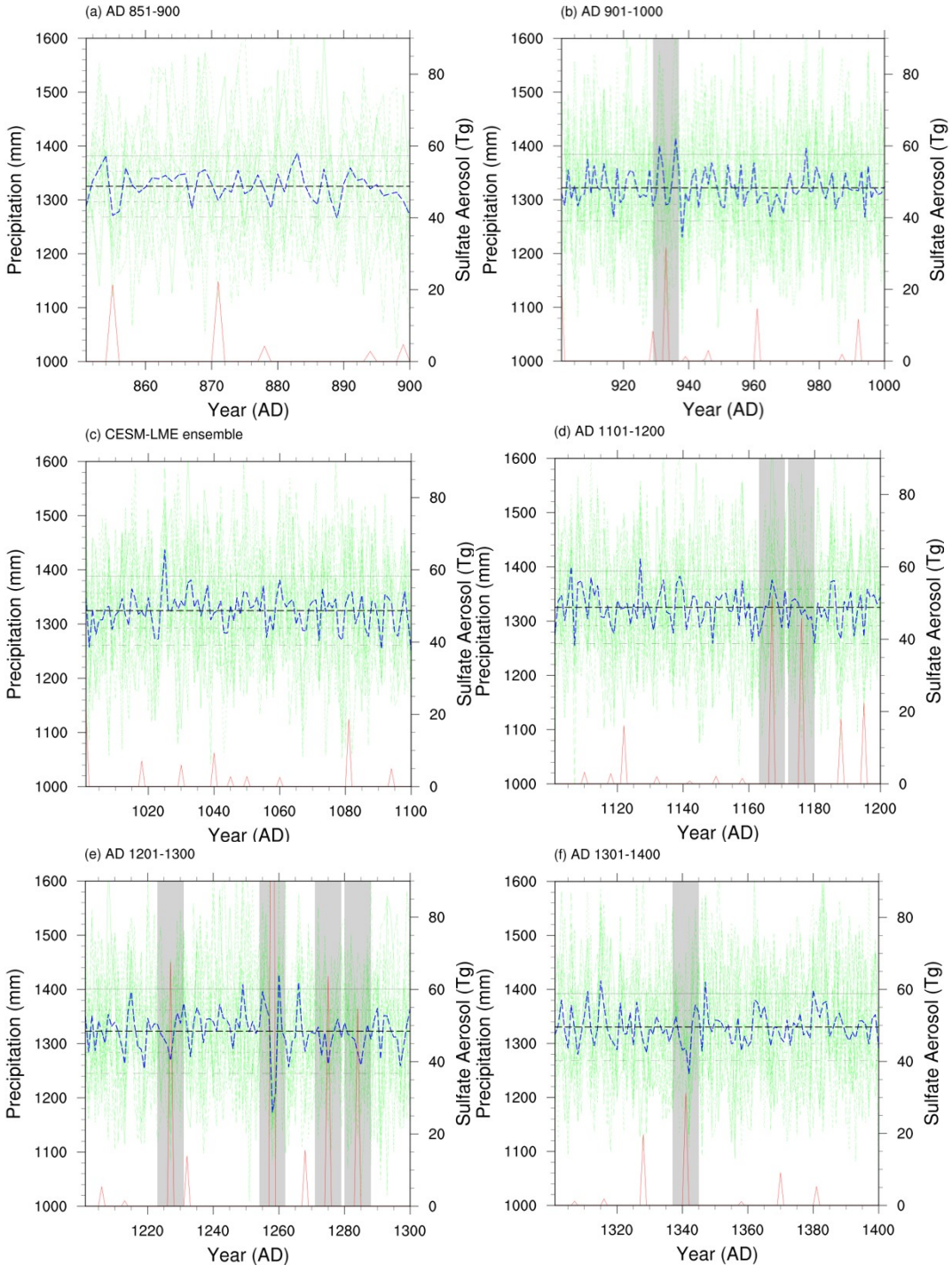
(a) AD 851-900
(b) AD 901-1000
(c) CESM-LME ensemble
(d) AD 1101-1200
(e) AD 1201-1300
(f) AD 1301-1400
Precipitation (mm)
Sulfate Aerosol (Tg)
Year (AD)

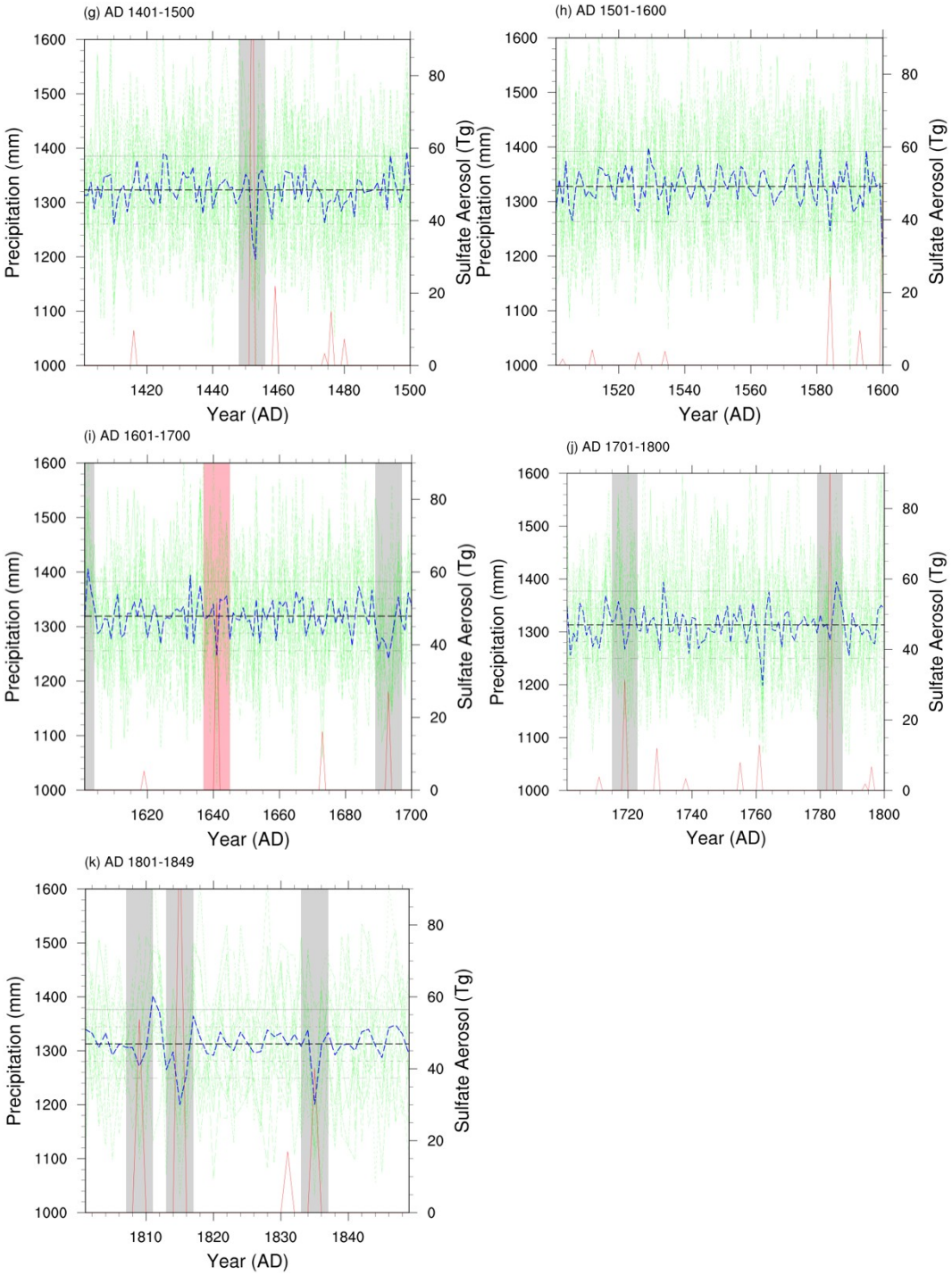

Fig. S2. (a) - (j) The ensemble mean precipitation anomaly (blue dashed lines) from AD 850-1850 simulated by CESM-LME (Otto-Bliesner et al.,2015) with its 13 ensemble members (green dashed lines). The red solid lines are the reconstructed volcanic sulphate aerosol (Gao et al., 2012). The black horizontal dashed lines in each figure mark the ±1 and ±2 standard deviations. The gray shaded area covers the period 4 years before and after the volcanic eruptions larger than 25Tg in the last millennium. The red shaded area covers the period of the Ming Dynasty Megadrought from 1637 to 1643.

Fig. S3

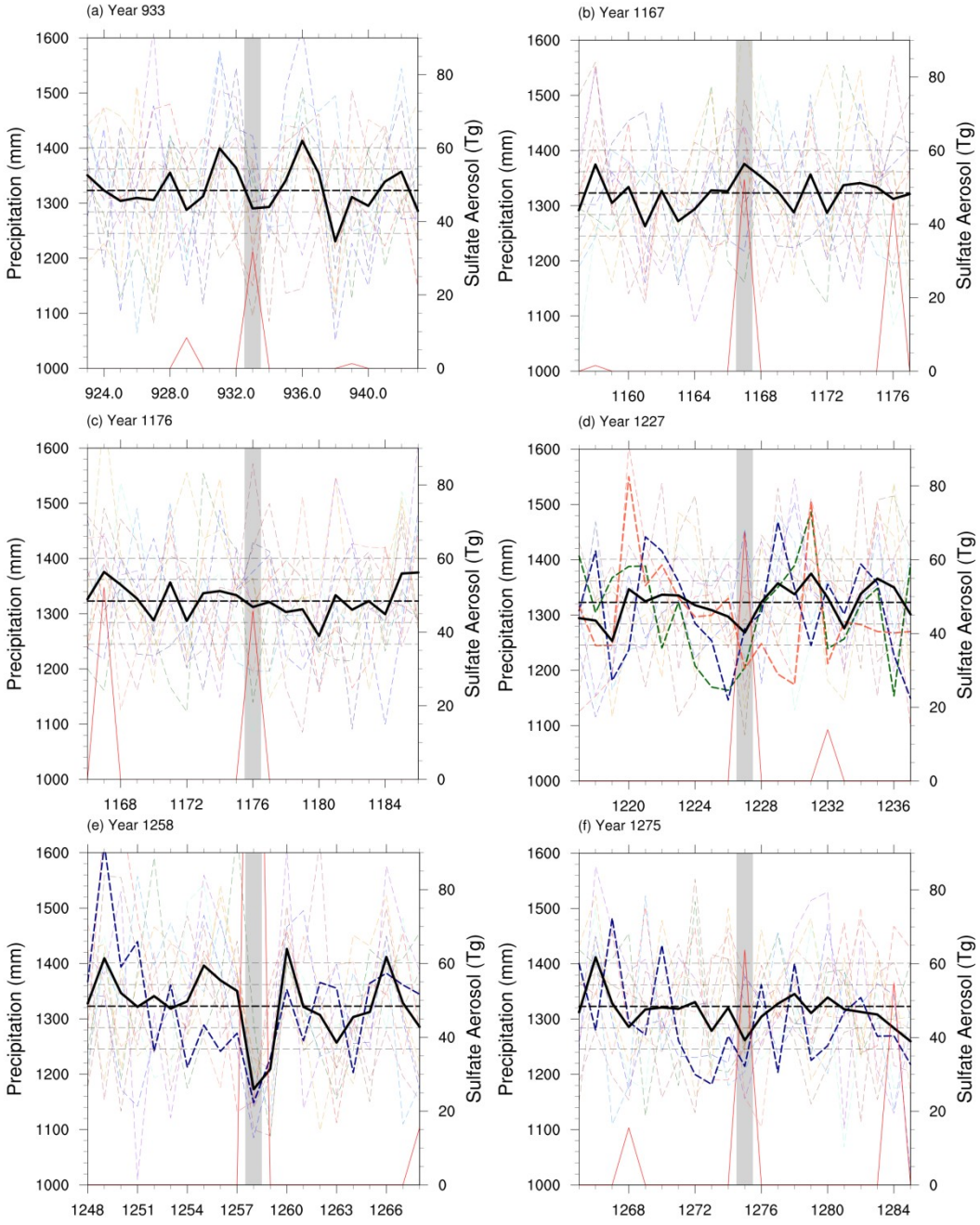
(a) Year 933
(b) Year 1167
(c) Year 1176
(d) Year 1227
(e) Year 1258
(f) Year 1275
Precipitation (mm)
Sulfate Aerosol (Tg)
1000
1100
1200
1300
1400
1500
1600
0
20
40
60
80
924.0
928.0
932.0
936.0
940.0
1160
1164
1168
1172
1176
1180
1184
1220
1224
1228
1232
1236
1248
1251
1254
1257
1260
1263
1266
1268
1272
1276
1280
1284

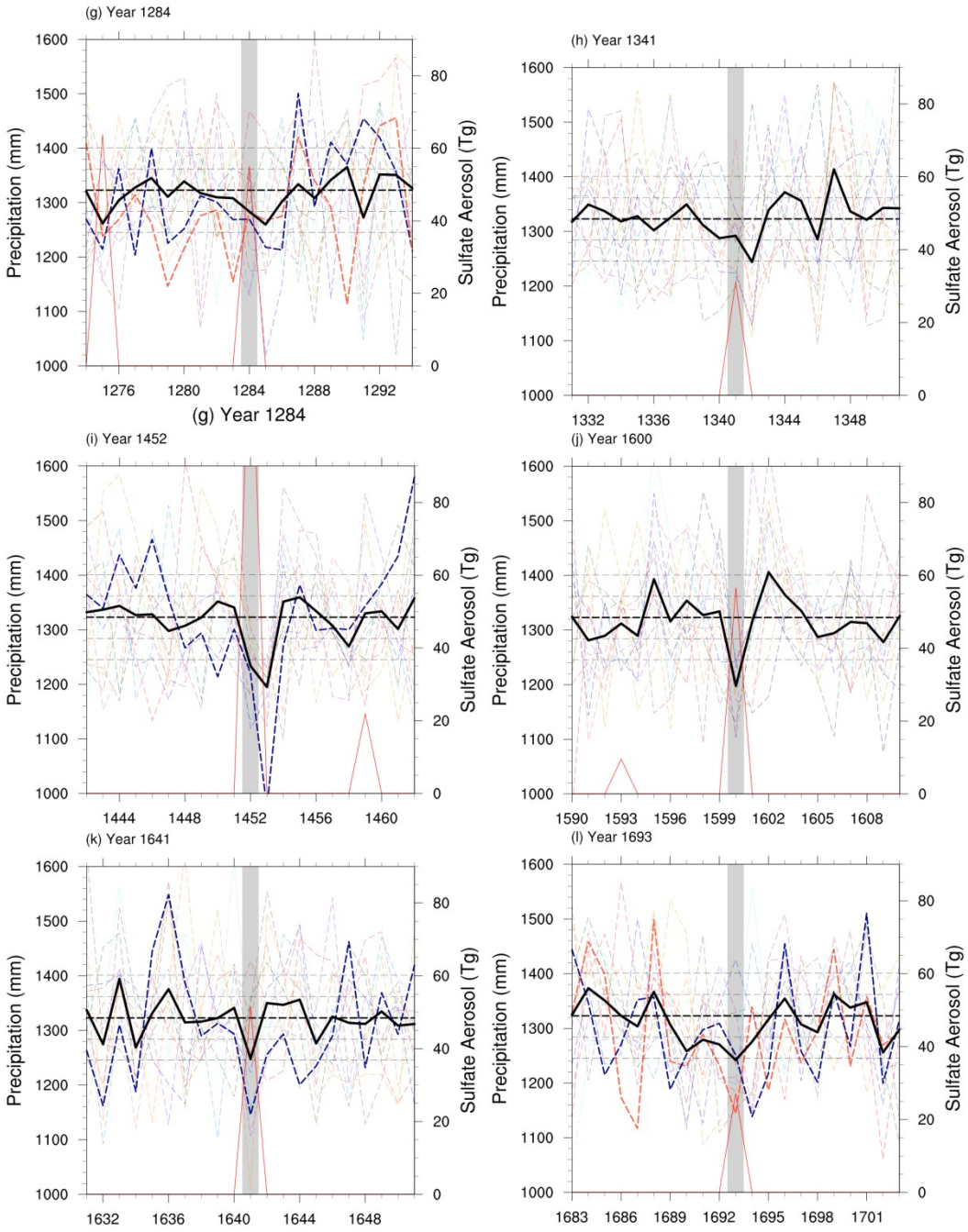
(g) Year 1284
(h) Year 1341
(i) Year 1452
(j) Year 1600
(k) Year 1641
(l) Year 1693
Precipitation (mm)
Sulfate Aerosol (Tg)
(g) Year 1284

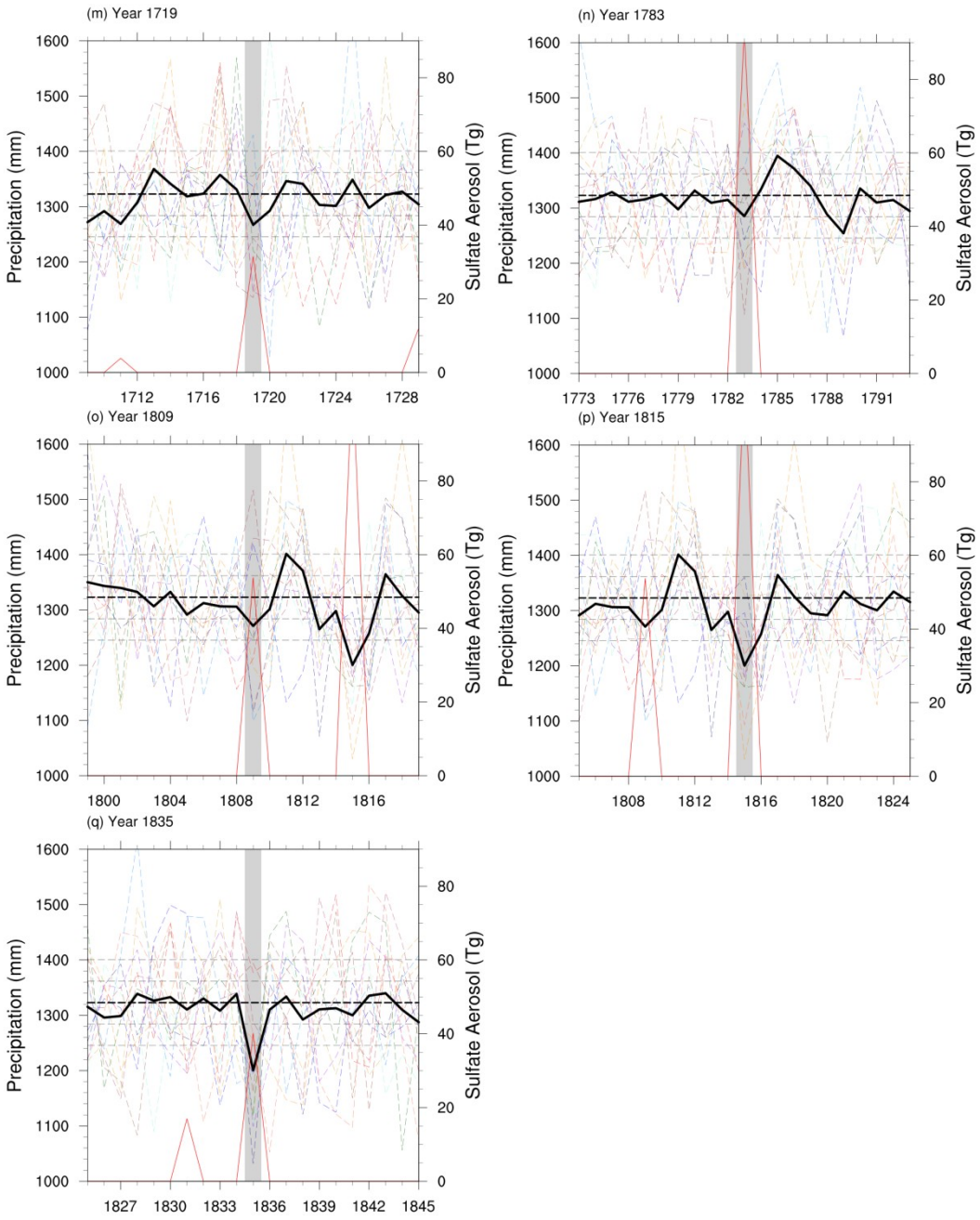

Fig. S3. The ensemble mean precipitation anomaly (black line) simulated by CESM-LME (Otto-Bliesner et al.,2015) and its 13 individual experiments (coloured dashed lines) centred with the 17 volcanic eruptions larger than 25Tg in 850-1850 (mentioned in Fig. S7) respectively. The bold coloured dashed lines are drought cases that persisted more than 3 years before the eruptions. The red solid lines are the reconstructed volcanic sulphate aerosol (Gao et al., 2012). The black dashed horizontal lines in each figure mark the ±1 and ±2 standard deviations.

Fig. S4

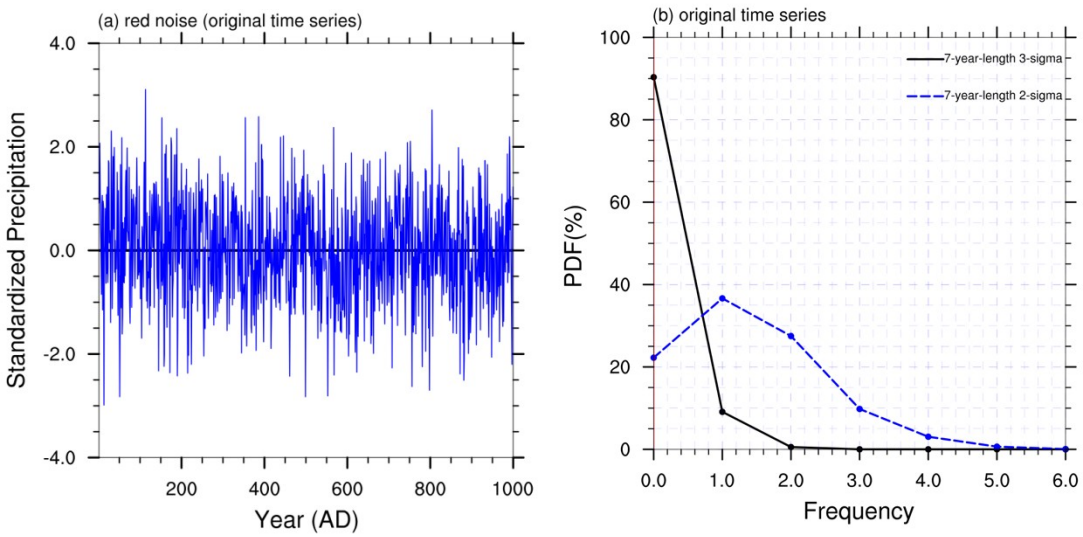

Fig. S4. (a) One sample of the red noise time series with one thousand year length for Monte Carlo test. (b) The Probability Distributions of drought frequencies based on the 2000-member red noise Monte Carlo simulations. The x-axis represents the number of drought events in a 1000-year red noise time series. The y-axis represents the percentage of drought frequency of the 2000 members. The solid black line is related to drought with 7-year length and above 3-sigma intensity, the dashed blue line is related to drought with 7-year length and above 2-sigma intensity.

Fig. S5

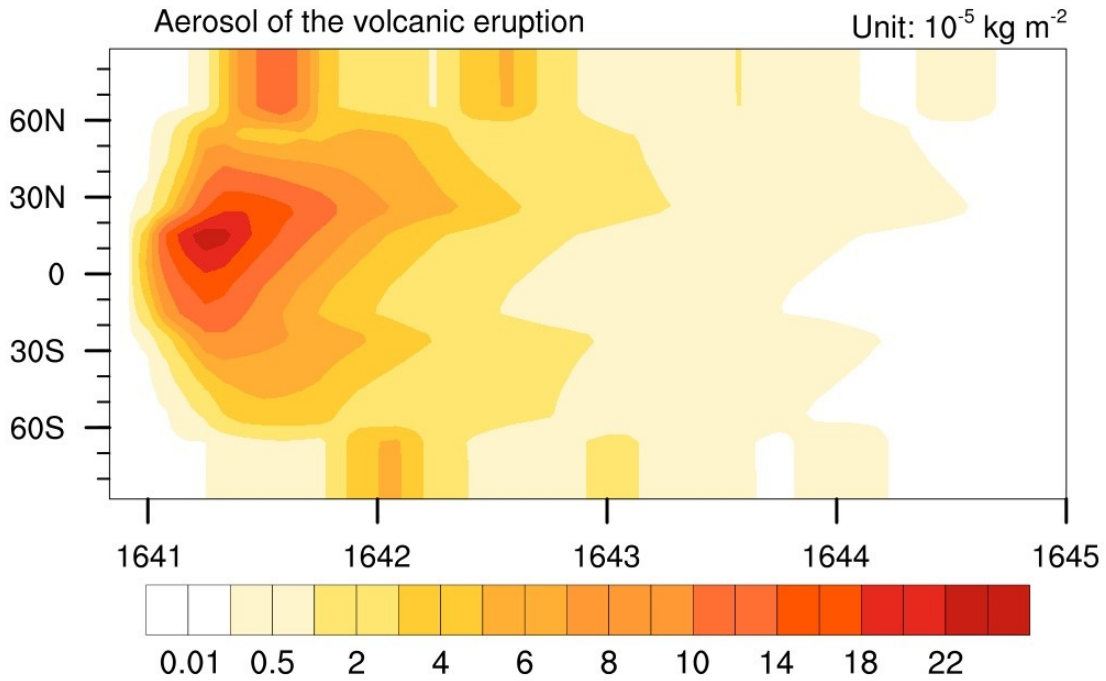

Fig. S5. The zonal-averaged evolution of sulphate aerosol (Gao et al., 2012) from 1641 MT. Parker volcanic eruption as external forcing (unit: 10-5kg/m2) used in the sensitivity experiment to reproduce the influences from volcanic eruptions on MDMD

Fig. S6

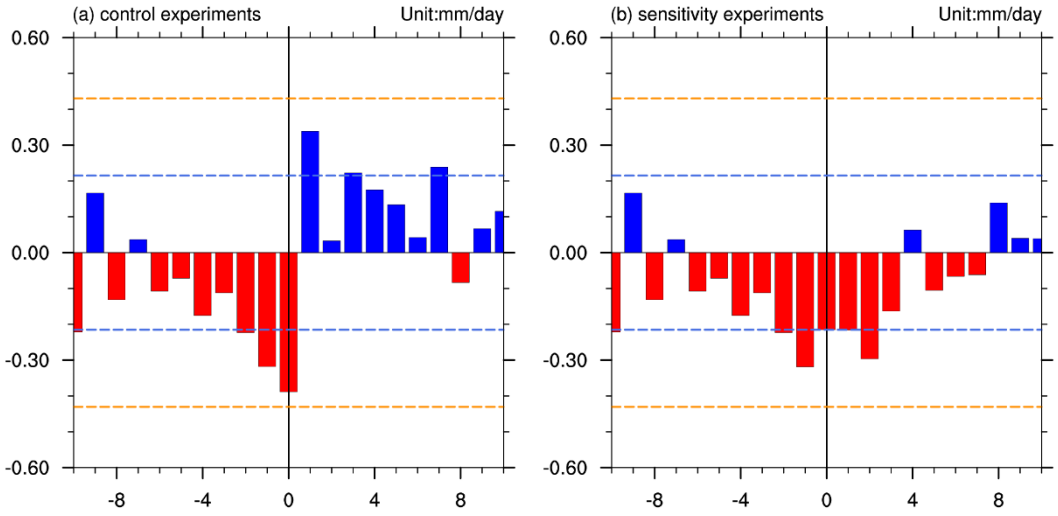

Fig. S6. The superposed echo analysis of the annual mean precipitation anomalies (Unit: mm/day) from the control experiments (a) and sensitivity experiments (b). The blue and yellow dashed lines in (a) and (b) indicate the ±0.5 and ±1 standard deviation, respectively.

Fig. S7

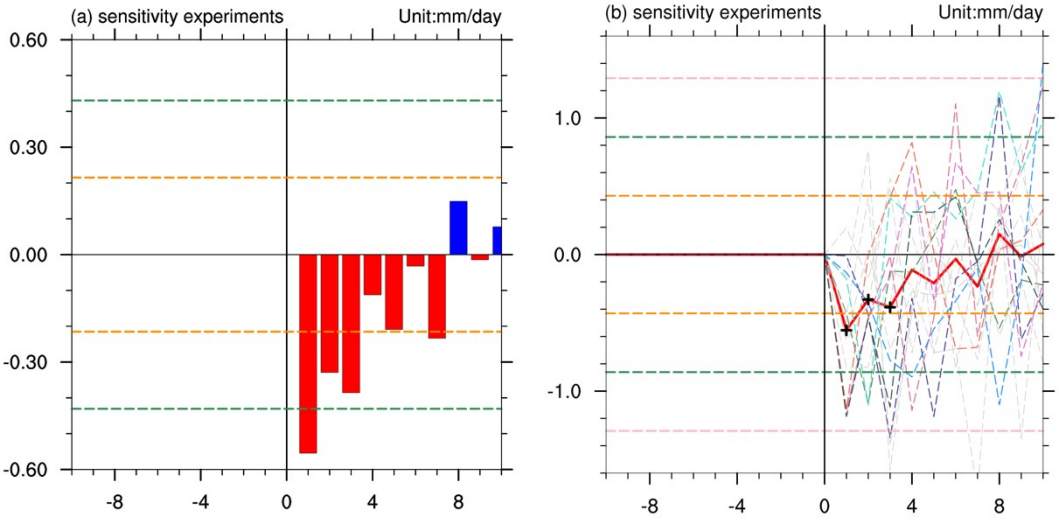

Fig. S7. The differences of precipitation (unit: mm/day) in sensitivity (a) and control (b) simulations in the same period. The yellow and green linesmark ±1 and ±2 standard deviation.
(b) is similar to (a) but with all ensemble members (dashed lines). The yellow, green and pink lines mark ±1, ±2 and ±3 standard deviation.

Fig. S8

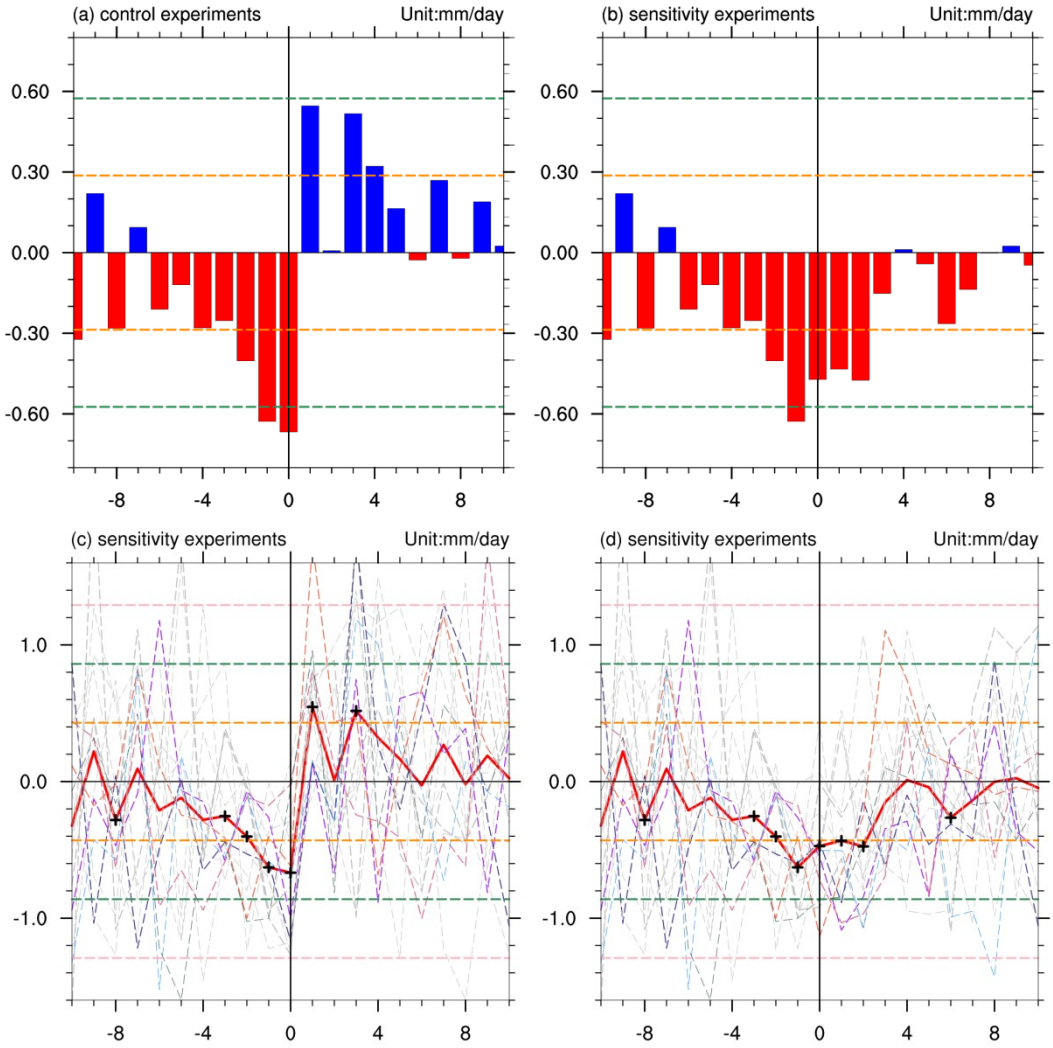

Fig. S8. The superposed echo analysis of the summer (MJJAS) averaged precipitation anomalies (unit: mm/day) from the control experiments (a) and sensitivity experiments (b)
(c), (d) is similar to (a), (b), but with all ensemble members (dashed lines, the thick colored dashed lines represent drought over 2 standard deviation, while thin gray dashed lines represent drought below 2 standard deviation). The "+" indicate that the anomalies are significant at 95% level based on student t-test. The blue and yellow dashed lines in (a) and (b) indicate the ±0.5 and ±1 standard deviation, respectively; the yellow, green and red dash lines in (c) and (d) indicate the ±1, ±2 and ±3 standard deviation, respectively.

Fig. S9

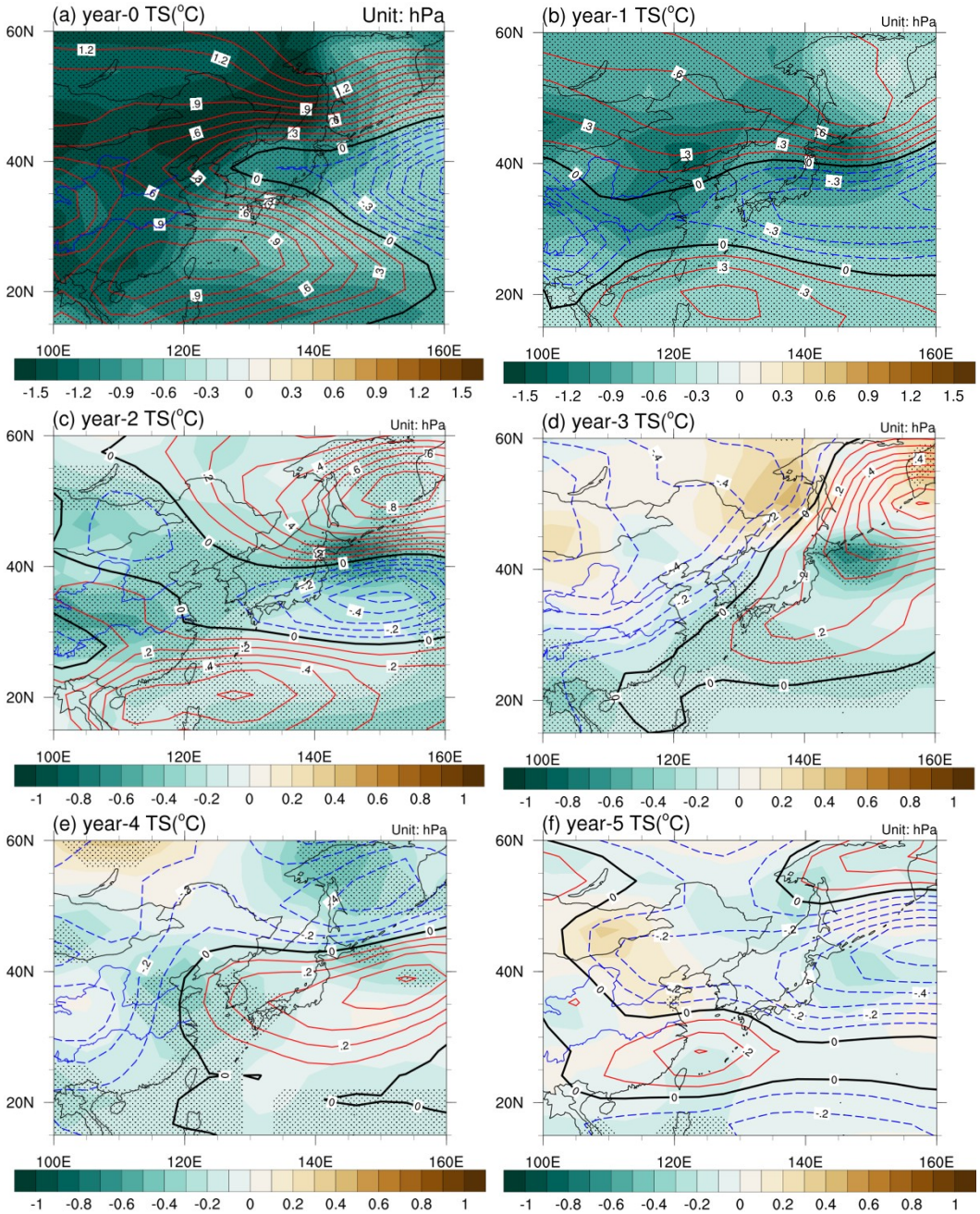

Fig. S9. (a) - (f) The ensemble mean anomalies of the summer (May to September) surface temperature (unit: ℃) and sea level pressure (blue dashed lines represent negative values while red dashed lines represent positive values, black lines are 0 value, unit: hPa) 6 years (year 0-5) after the eruption in the volcanic sensitivity experiments.

Fig. S10

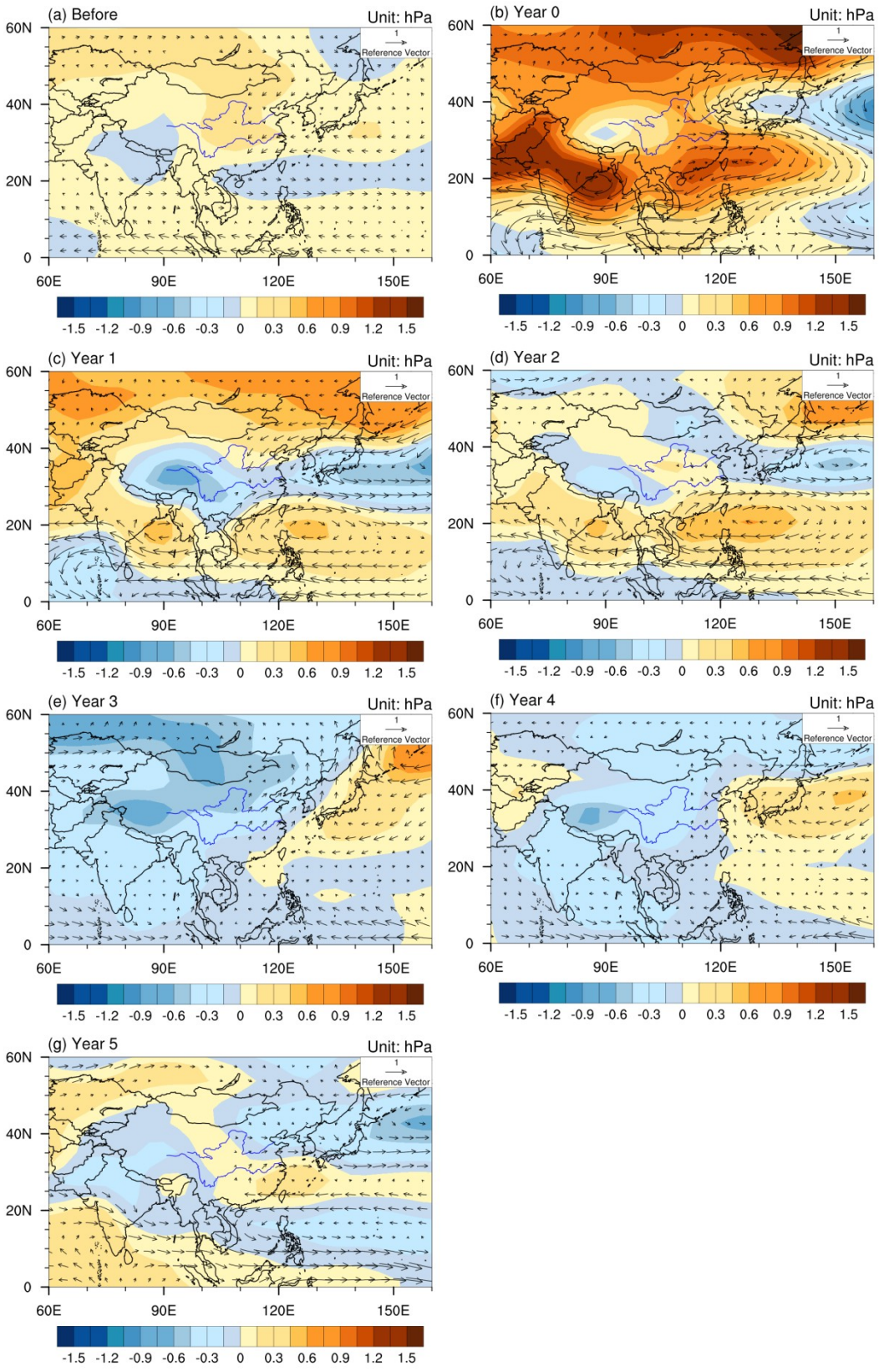
(a) Before
Unit: hPa
(b) Year 0
Unit: hPa
(c) Year 1
Unit: hPa
(d) Year 2
Unit: hPa
(e) Year 3
Unit: hPa
(f) Year 4
Unit: hPa
(g) Year 5
Unit: hPa
Reference Vector
60N
40N
20N
0
60E
90E
120E
150E
-1.5 -1.2 -0.9 -0.6 -0.3 0 0.3 0.6 0.9 1.2 1.5

Fig. S10. The ensemble mean anomalies of the summer (May to September) Sea Level Pressure (SLP, unit: hPa) and 850-hPa wind field (unit: m/s) in the 6 years prior to the volcanic eruption (a, year -6--1) and 6 years after the eruption (year 0-5) in the volcanic sensitivity experiments (b-g) .

Fig. S11

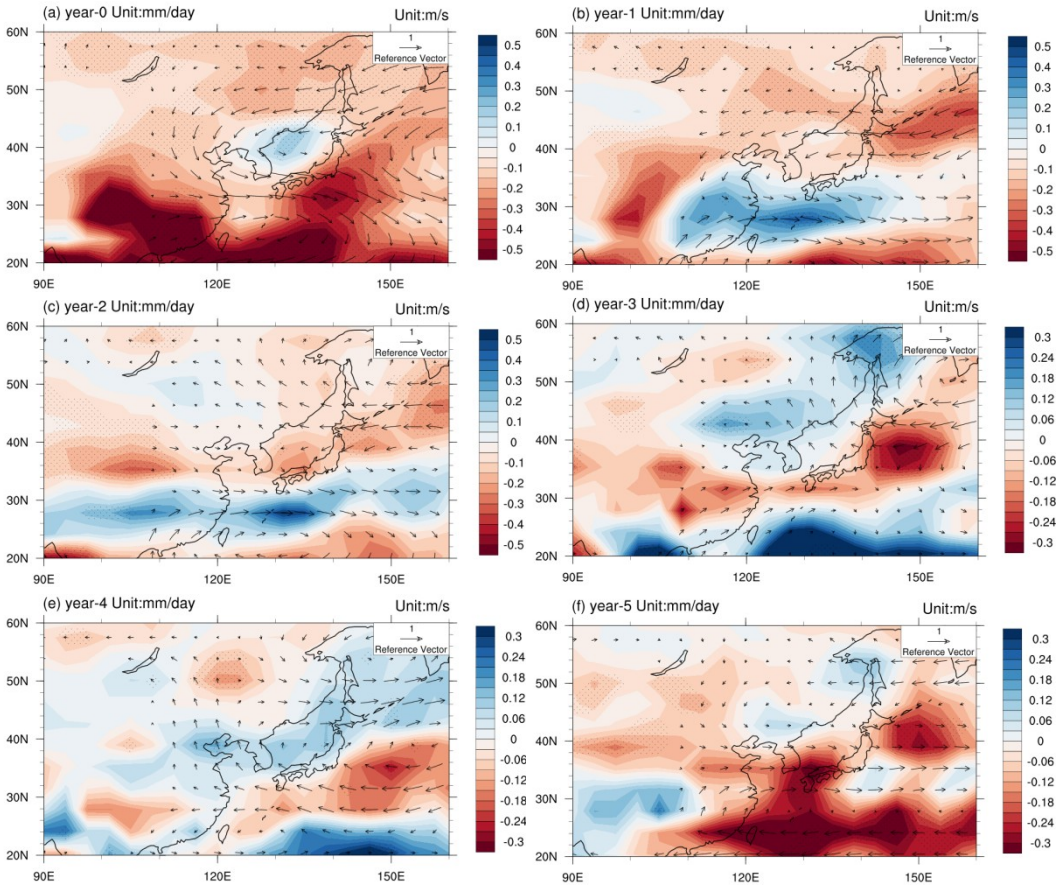

Fig. S11. (a) - (f) The ensemble mean anomalies of summer (May to September) precipitation (unit: mm/day) and 850-hPa wind (unit: m/s) 6 years after the eruption (year 0-5) in the volcanic sensitivity experiments.

Fig. S12.

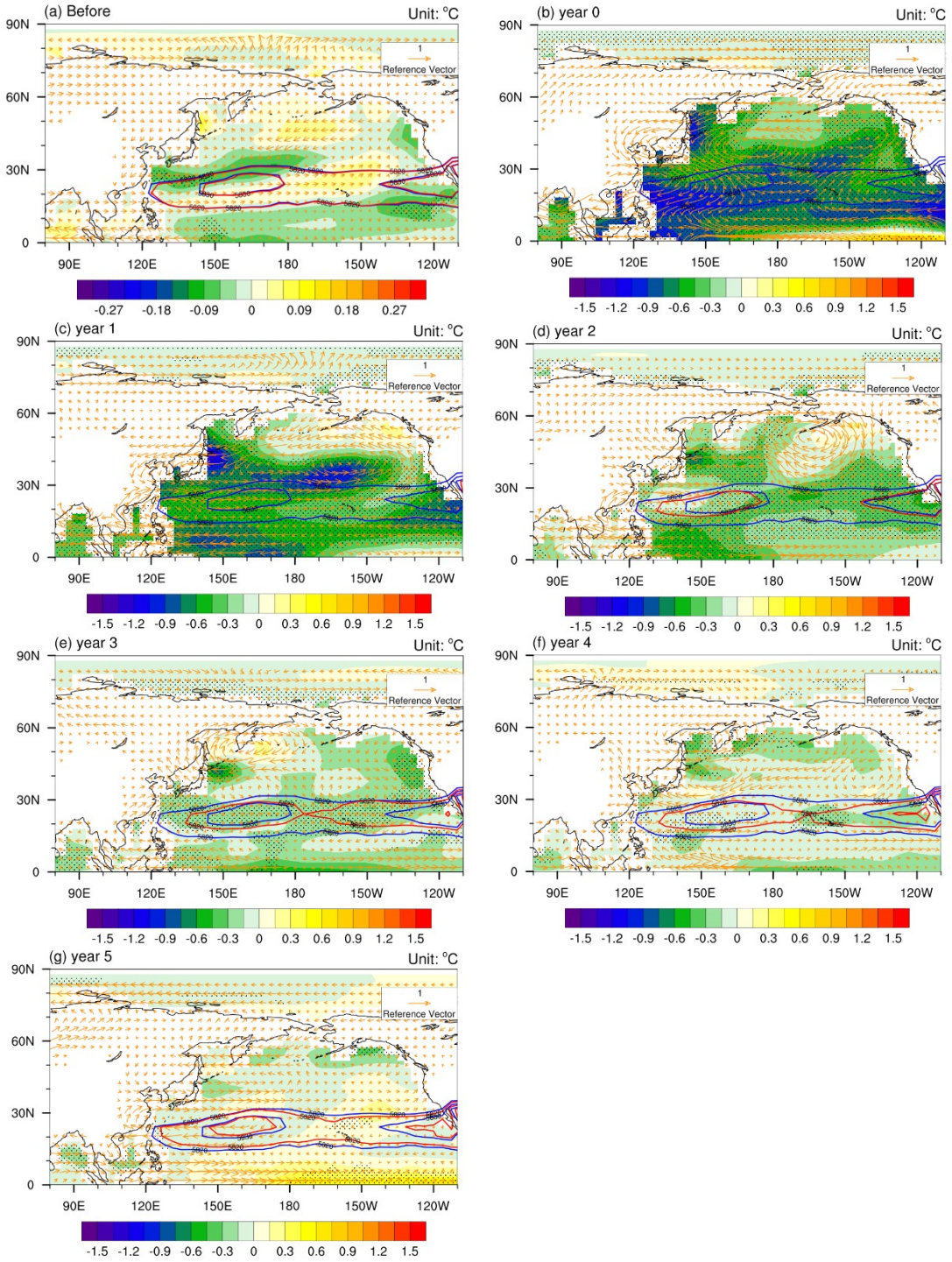

Fig. S12. (a) - (g) The ensemble mean global summer (May to September) Sea Surface Temperature Anomaly (SSTA) (unit: °C) before the volcanic eruption (a, mean of the SST from year -5 to -1) and 6 years after the explosion (b-g). The dots denote areas with confidence levels exceeding 95%. The yellow arrows are the anomalies of summer (May to September) 850-hPa wind (unit: m/s). The red lines are the 500-hPa Geopotential Height contour line (unit: gpm). The blue line is the climatology of the 500-hPa Geopotential Height. Year 0 is the eruption year.

Fig. S13

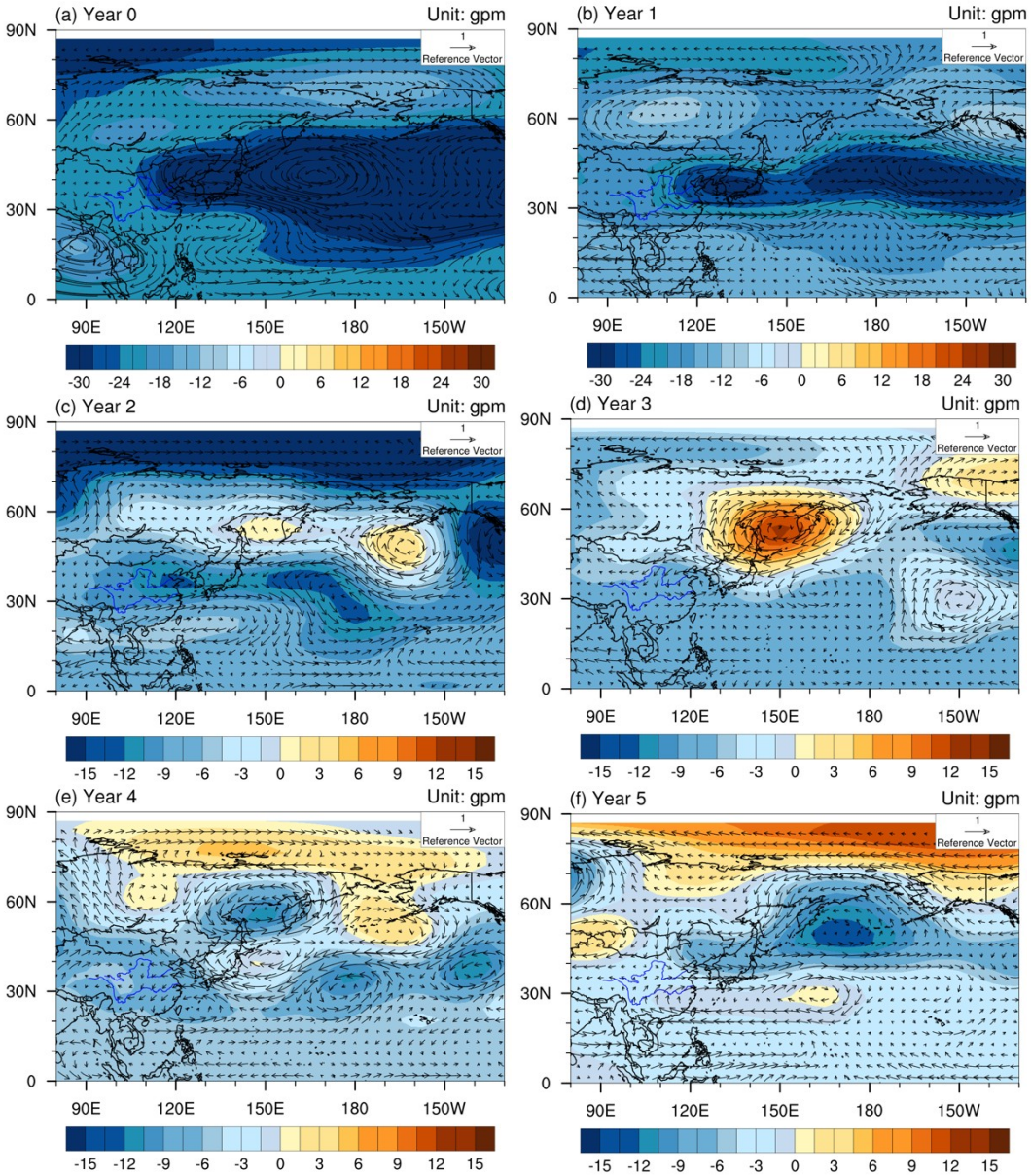

Fig. S13. (a) - (f) The ensemble mean anomalies of the summer (May to September) 500hPa geopotential height (unit: gpm) and 500hPa wind (unit: m/s) 6 years after the eruption (year 0-5) in the volcanic sensitivity experiments.

Fig. S14

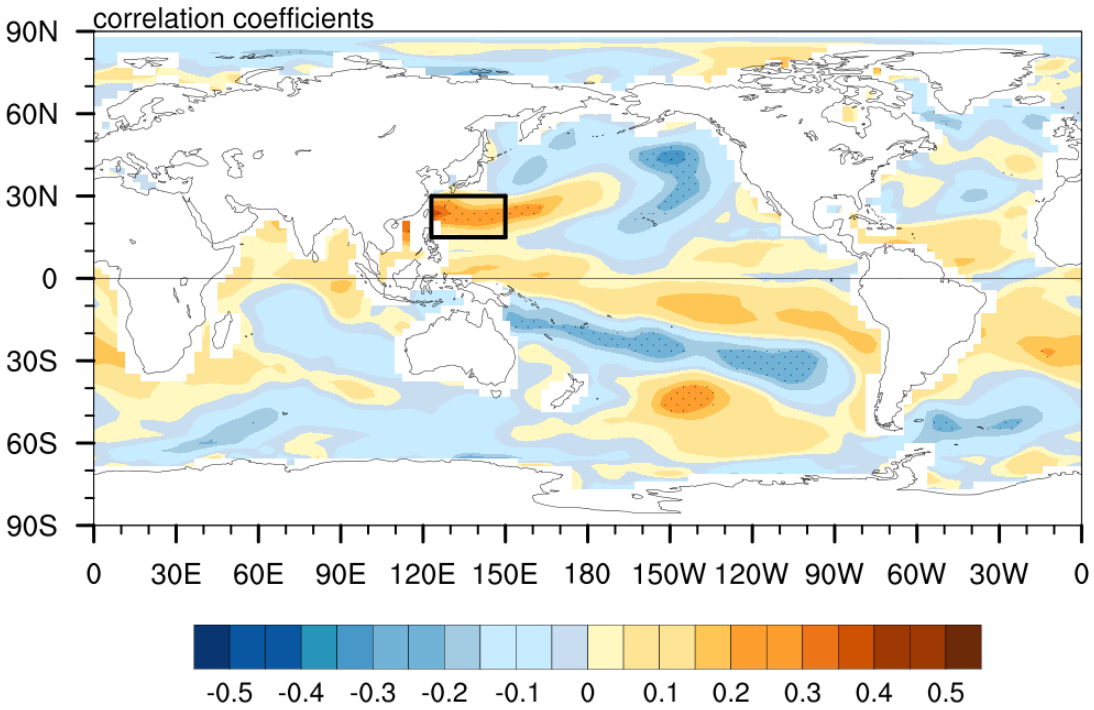

Fig. S14. The correlation coefficients between the summer (MJJAS) precipitation over the eastern China and SST in the control experiment. The stippling indicate the correlation coefficients are significant at 95% level. The region in black rectangle is 123°E-150°E, 15°N-30°N.

SI References

1. Otto-Bliesner, B. L. *et al.* Climate Variability and Change since 850 C.E.: An Ensemble Approach with the Community Earth System Model (CESM). *Bulletin of the American Meteorological Society* **97**, 150807114607005, doi:10.1175/BAMS-D-14-00233.1 (2015).
2. Gao, C., Robock, A. & Ammann, C. Volcanic forcing of climate over the past 1500 years: An improved ice. *Journal of Geophysical Research* **117**, D16112, doi:10.1029/2008JD010239 (2012)